M-BAND DUAL TREE COMPLEX WAVELET TRANSFORM FOR TEXTURE IMAGE INDEXING AND RETRIEVAL

K. N. Prakash[1] and K. Satya Prasad[2]
[1]Research Scholar, [2]Rector &Professor
Department of Electronics and Communication Engineering
Jawaharlal Nehru Technological University, Kakinada
Andhra Pradesh, India

ABSTRACT

A new set of two-dimensional (2-D) M-band dual tree complex wavelet transform (M_band_DT_CWT) is designed to improve the texture retrieval performance. Unlike the standard dual tree complex wavelet transform (DT_CWT), which gives a logarithmic frequency resolution, the M-band decomposition gives a mixture of a logarithmic and linear frequency resolution. Most texture image retrieval systems are still incapable of providing retrieval result with high retrieval accuracy and less computational complexity. To address this problem, we propose a novel approach for texture image retrieval using M_band_DT_CWT by computing the energy, standard deviation and their combination on each subband of the decomposed image. To check the retrieval performance, texture database of 1856 textures is created from Brodatz album. Retrieval efficiency and accuracy using proposed features is found to be superior to other existing methods.

KEYWORDS: *M-band wavelets; Feature Extraction; M-band dual tree complex wavelets; Image Retrieval*

I. INTRODUCTION

A. Motivation

With the rapid expansion of worldwide network and advances in information technology there is an explosive growth of multimedia databases and digital libraries. This demands an effective tool that allow users to search and browse efficiently through such a large collections. In many areas of commerce, government, academia, hospitals, entertainment, and crime preventions large collections of digital images are being created. Usually, the only way of searching these collections was by using keyword indexing, or simply by browsing. However, as the databases grew larger, people realized that the traditional keywords based methods to retrieve a particular image in such a large collection are inefficient. To describe the images with keywords with a satisfying degree of concreteness and detail, we need a very large and sophisticated keyword system containing typically several hundreds of different keywords. One of the serious drawbacks of this approach is the need of trained personnel not only to attach keywords to each image (which may take several minutes for one single image) but also to retrieve images by selecting keywords, as we usually need to know all keywords to choose good ones. Further, such a keyword based approach is mostly influenced by subjective decision about image content and also it is very difficult to change a keyword based system afterwards. Therefore, new techniques are needed to overcome these limitations. Digital image databases however, open the way to content based searching. It is common phrase that an image speaks thousands of words. So instead of manual annotation by text based keywords, images should be indexed by their own visual contents, such as color, texture and shape. The main advantage of this method is its ability to support the visual queries. Hence researchers turned attention to content based image retrieval (CBIR) methods. The challenge in image retrieval is to find out features that capture the important characteristics of an image, which make it unique, and allow its accurate identification. Comprehensive and extensive literature survey on CBIR is presented in [1]–[4].

The texture features currently in use are mainly derived from multi-scale approach. Liu and Picard [5] have used Wold features for image modeling and retrieval. In SaFe project, Smith and Chang [6] used discrete wavelet transform (DWT) based features for image retrieval. Ahmadian et al. used the wavelet transform for texture classification [7]. Do et al. proposed the wavelet transform (DWT) based texture image retrieval using generalized Gaussian density and Kullback-Leibler distance (GGD &KLD) [8]. Unser used the wavelet frames for texture calsification and segmentation [9]. Manjunath et al. [10] proposed the Gabor transform (GT) for image retrieval on Bordatz texture database. They have used the mean and standard deviation features from four scales and six directions of Gabor transform. Kokare et al. used the rotated wavelet filters [11], dual tree complex wavelet filters (DT-CWF), dual tree rotated complex wavelet filters (DT-RCWF) [12], rotational invariant complex wavelet filters [13] for texture image retrieval. They have calculated the characteristics of image in different directions using rotated complex wavelet filters. Birgale et al. [14] and Subrahmanyam et al. [15] combined the color (color histogram) and texture (wavelet transform) features for CBIR.

B. Related Work

A drawback of standard wavelets is that they are not suitable for the analysis of high-frequency signals with relatively narrow bandwidth. Kokare et al. [16] used the decomposition scheme based on M-band wavelets, which yields improved retrieval performance. Unlike the standard wavelet decomposition, which gives a logarithmic frequency resolution, the M-band decomposition gives a mixture of a logarithmic and linear frequency resolution. Further as an additional advantage, M-band wavelet decomposition yields a large number of subbands, which improves the retrieval accuracy. One of the drawbacks with M-band wavelet in content-based image retrieval is that computational complexity increases and hence retrieval time with number of bands. Gopinath and Burrus [17] introduced Cosine-modulated class of multiplicity M wavelet tight frames (WTF's). In these WTF's, the scaling function uniquely determines the wavelets. This is in contrast to general multiplicity M case, where one has to, for any given application, design the scaling function and the wavelets. Hsin [16] used a modulated wavelet transform approach for texture segmentation and reported that texture segmentation performance can be improved with this approach. Guillemot and Onno [19] had used Cosine-modulated wavelet for image compression. They have presented procedure for designing Cosine-modulated wavelets for arbitrary length filters. This procedure allows obtaining filters with high stopband attenuation even in the presence of additional regularity constraints. Their results show that these filter solution provide good performance in image compression. The advantages of the Cosine-modulated wavelet are their low design and implementation complexities, good filter quality, and ease in imposing the regularity conditions, which yields improved retrieval performance both in terms of accuracy and retrieval time.

C. Main Contribution

The main contributions of this paper are summarized as follows. First, in this paper we have presented novel texture features for content-based image retrieval using M-band DT_CWT. Second, our approach of using the d1 distance metric for similarity measurement improves the retrieval performance from 62.26% to 75.54% compared with the traditional Euclidean distance metric (where same features were used but Euclidean distance metric is used for similarity measurement). This shows that good performance in retrieval comes not just from a good set of features but also together with the use of suitable similarity measurement, which supports our approach.

The organization of the paper as follows: In section I, a brief review of image retrieval and related work is given. Section II, presents a concise review of M-band DT_CWT. Section III, presents the feature extraction and similarity measure. Experimental results and discussions are given in section IV. Based on above work conclusions are derived in section V.

II. M- CHANNEL FILTER BANK

The structure of the classical one-dimensional filter bank is depicted in Fig. 1. The input signal *x(n)* is filtered by a set of M filters $h_i(n)$. The desired filter responses are shown in Fig.2. The response of the i^{th} filter occupies only a subband of [−π , π]. Subband signals are down sampled by M to give the signal $d_i(n)$. At the reconstruction side these subband signals are passed through $g_i(n)$ and up sampled by M to get output signal *y(n)*. The filters $h_i(n)$ are analysis filters constituting the analysis filter bank and the filters $g_i(n)$ are the synthesis filters constituting the synthesis filter bank. Perfect reconstruction of the signal is an important requirement of M-Channel filter bank. Filter bank is said to be perfect reconstruction if *y(n) = x(n)*. Under certain conditions, perfect reconstruction filter banks are associated with wavelet frames for $L^2(R)$ [17]. This association is a correspondence between the filters and scaling and wavelet vectors associated with the wavelet frames.

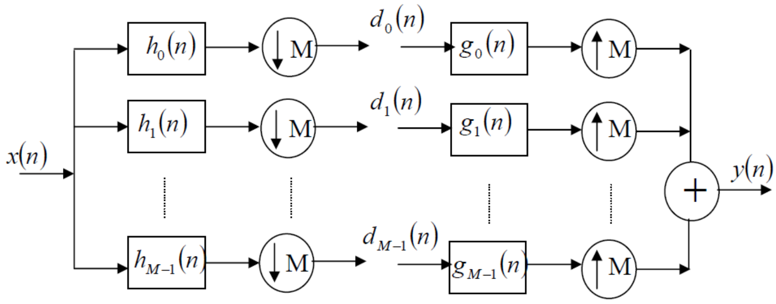

Fig. 1: M- Channel filter bank

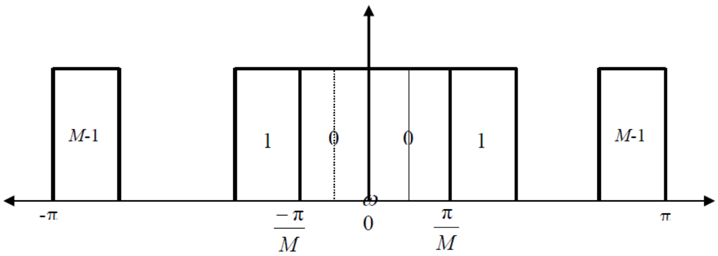

Fig. 2: Ideal frequency responses in M channel filter bank

A. Dual Tree Complex Wavelet Transform (DT_CWT)

The 1-D DT-CWT decomposes a signal $f(t)$ in terms of a complex shift and dilated mother wavelet $\psi(t)$ and scaling function $\phi(t)$

$$f(t) = \sum_{l \in Z} s_{j_0,l}\phi_{j_0,l}(t) + \sum_{j \geq j_0}\sum_{l \in Z} c_{j,l}\psi_{j,l}(t) \tag{1}$$

Where $s_{j_0,l}$ is scaling coefficient and $c_{j,l}$ is complex wavelet coefficient with ϕ_{j_0} and $\psi_{j,l}$ complex: $\phi_{j_0} = \phi^r_{j_0,l} + i\phi^i_{j_0,l}$, $\psi_{j_0} = \psi^r_{j_0,l} + i\psi^i_{j_0,l}$. The $\psi^r_{j_0,l}$ and $\psi^i_{j_0,l}$ are themselves real wavelets: the complex wavelet transform is combination of two real wavelet transforms. Fig. 3 shows that the implementation of 1-D DT-CWT.

2-D DT-CWT can be implemented using separable wavelet transforms like 2-D wavelet transform. Impulse responses of six wavelets associated with 2-D complex wavelet transform is illustrated in Fig. 4. These six wavelet sub-bands of the 2-D DT-CWT are strongly oriented in $\{+15^0, +45^0, +75^0, -15^0, -45^0, -75^0\}$ direction and captures image information in that direction. Frequency domain partition of DT-CWT resulting from two level decomposition is shown in Fig. 5.

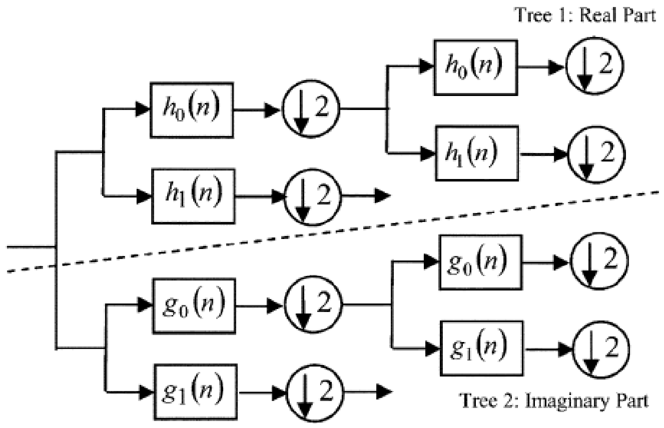

Fig. 3: 1-D dual- tree complex wavelet transform

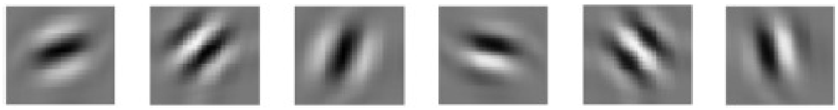

Fig. 4: Impulse response of six wavelet filters of DT-CWT

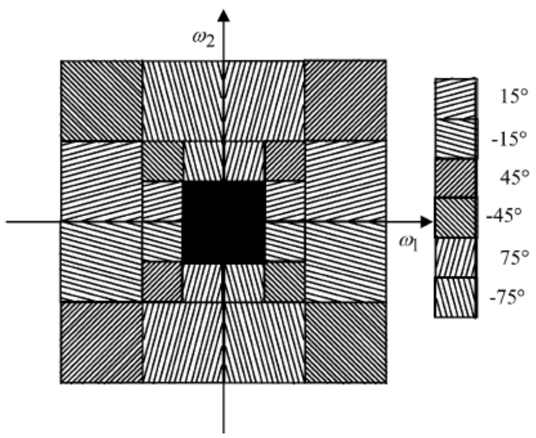

Fig. 5: Frequency domain partition in DT-CWT resulting from two level decomposition.

B. M- Band Wavelet

There is a close relationship between M-band wavelets and M-channel filter banks [17]. M-band wavelets are a generalization of the conventional wavelets reported in the literature [20], [21]. Disadvantage of using standard wavelets is that they are not suitable for the analysis of high-frequency signals with relatively narrow bandwidth [5]. To overcome this problem M-band orthonormal wavelet were developed. M-band was developed by generalizing the two band wavelet, which was designed by Daubechies [22]. The M-band orthonormal wavelets give a better energy compaction than two band wavelets by zooming into narrow band high frequency components of a signal [23].

In M-band wavelets there are M-1 wavelets $\psi_l(x), l = 1,2,....,M-1,$ which form the basis functions and are associated with the scaling functions. The M-band wavelet system forms a tight frame for the set of square integrable functions defined over the set of real numbers $(L^2(R))$ [17]. A function $f(x) \in (L^2(R))$ is represented by

$$f(x) = \sum_{l=1}^{M-1} \sum_{m \in Z} \sum_{n \in Z} \left\langle f(x), \psi_{l,m,n}(x) \right\rangle \psi_{l,m,n}(x) \tag{2}$$

where Z represents the set of integers and . $\langle . \rangle$ is an inner product. $\psi_l(x)$ is scaled and translated to obtain $\psi_{l,m,n}(x)$ functions [17].

$$\psi_{l,m,n}(x) = M^{m/2}\psi_l(M^{m/2}x - n) \quad l = 1,2,....,M-1, m \in Z, n \in Z \tag{3}$$

Gopinath and Burrus [22] have shown that the wavelet functions $\psi_l(x)$ are defined from a unique, compactly supported scaling function $\psi_0(x) \in L^2(R)$ with support in [0, (N −1) (M −1)] by

$$\psi_l(x) = \sqrt{M}\sum_{n=0}^{N-1} h_l(x)\psi_0(Mx - n); \quad l = 1,2,....,M-1 \tag{4}$$

The scaling function satisfies the recursion equation:

$$\psi_0(x) = \sqrt{M}\sum_{n=0}^{N-1} h_0(x)\psi_0(Mx - n); \tag{5}$$

Where h_0 is a scaling filter of length $N = M*K$ (K is regularity of scaling function), which satisfies the following constraints.

$$\sum_{n=0}^{N-1} h_0(n) = \sqrt{M} \tag{6}$$

$$\sum_{n=0}^{N-1} h_0(n)h_0(n + Mi) = \delta(i) \tag{7}$$

The $(M-1)h_l$ filters are also of length N and are called the wavelet filters and satisfy the equation

$$\sum_{n=0}^{N-1} h_l(n)h_m(n + Mi) = \delta(i)\delta(l - m) \tag{8}$$

C. M-Band DT_CWT

The dual tree complex wavelet (DT_CWT), which was originally developed using two 2-band DWTs was extended to M-band DWTs recently in [24], and used for image processing in [25]. The M-band DT_CWT in [24, 25] employes two M-band DWTs where the wavelets associated with the two transforms from Hilbert transform pairs.

A typical M-Band DT_CWT analysis filter bank for M=4 is shown in Fig. 6. The filter bank in essence is a set of bandpass filters with frequency and orientation selective properties. In the filtering stage we make use of biorthonormal M-band DT_CWT to decompose the texture image into M×M-channels, corresponding to different direction and resolutions. The one dimensional *M (=4)*-band wavelet filter impulse responses are given by ψ_l and their corresponding transfer functions are denoted by h_l for *l=0, 1, 2, 3.* ψ_1 is the scaling function (lowpass filter) and other ψ_l's correspond to the wavelet functions (bandpass filters). In this work we have obtained the

M channel 2-D separable transform by the tensor product of M-band 1-D DT_CWT filters. At each level with M=4, the image is decomposed in to M×M (=16) channels. Table I shows the 4-band dual tree wavelet filter coefficients [16] used in the experiments.

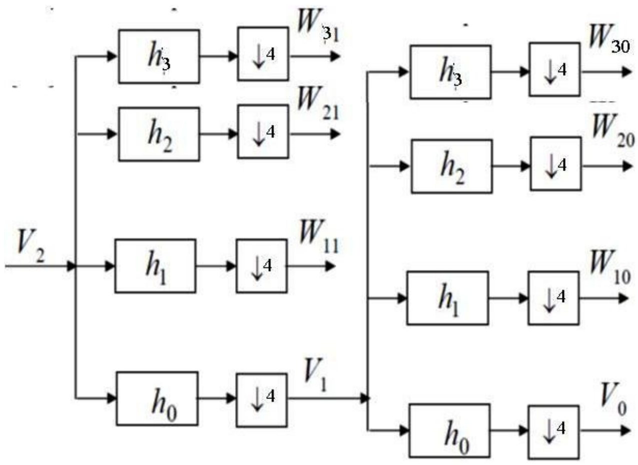

Fig. 6: M- Band (M=4) wavelet filter bank structure

TABLE I Three band Dual Tree Complex Wavelet Filter Coefficients used in Experiments.

h_0	h_1	h_2	h_3
0.030550699	0.01990811	0.01990811	0.030550699
-0.01990811	-0.030550699	0.030550699	0.01990811
-0.058475205	-0.038104884	-0.038104884	-0.058475205
-0.038104884	-0.058475205	0.058475205	0.038104884
-0.036706282	-0.168841015	-0.168841015	-0.036706282
0.168841015	0.036706282	-0.036706282	-0.168841015
0.4095423	0.544260466	0.544260466	0.4095423
0.544260466	0.4095423	-0.4095423	-0.544260466
0.544260466	-0.4095423	-0.4095423	0.544260466
0.4095423	-0.544260466	0.544260466	-0.4095423
0.168841015	-0.036706282	-0.036706282	0.168841015
-0.036706282	0.168841015	-0.168841015	0.036706282
-0.038104884	0.058475205	0.058475205	-0.038104884
-0.058475205	0.038104884	-0.038104884	0.058475205
-0.01990811	0.030550699	0.030550699	-0.01990811
0.030550699	-0.01990811	0.01990811	-0.030550699

III. FEATURE EXTRACTION

Each image from the database was analyzed using M_band_DT_CWT. The analysis was performed up to third level (16×3×2=96 subbands) of the wavelet decomposition. For constructing the feature vector feature parameters such as energy, standard deviation and combinations of both were computed separately on each subband and are stored in vector form. The basic assumption of this approach is that the energy distribution in the frequency domain identifies a texture. Besides providing acceptable retrieval performance from large texture, this approach is partly supported by physiological studies of the visual cortex as reported by Hubel and Wiesel [26] and Daugman [27]. The energy and standard deviation of decomposed subbands are computed as follows:

$$Energy = E_k = \frac{1}{M \times N}\sum_{i=1}^{M}\sum_{j=1}^{N}\left|W_{ij}\right| \tag{9}$$

$$Standard\ Deviation = \sigma_k = \left[\frac{1}{M \times N} \sum_{i=1}^{M} \sum_{j=1}^{N} (W_{ij} - \mu_{ij})^2 \right]^{1/2} \quad (10)$$

where W_{ij} is the wavelet-decomposed subband, M×N is the size of wavelet-decomposed subband, k is the number of subbands (k=18 for two levels), and μ_{ij} is the subband mean value.

A feature vector is now constructed using E_k and σ_k as feature components. Length of feature vector will be equal to (No. of subbands × No. of feature parameters used in combination) elements. Resulting feature vectors are as follows:

Using only energy feature measure

$$\overline{f}_E = [E_1, E_2, ...E_k] \quad (11)$$

Using only standard deviation feature measure

$$\overline{f}_\sigma = [\sigma_1, \sigma_2, ...\sigma_k] \quad (12)$$

Using combination of standard deviation and energy feature measure

$$\overline{f}_\sigma = [\sigma_1, \sigma_2, ...\sigma_k\ E_1, E_2, ...E_k] \quad (13)$$

For creation of feature database above procedure is repeated for all the images of the image database and these feature vectors are stored in feature database.

A. Similarity Distance Measure

In the presented work d_1 similarity distance metric is used as shown below:

$$D(Q, I_1) = \sum_{i=1}^{Lg} \left| \frac{f_{I,i} - f_{Q,i}}{1 + f_{I,i} + f_{Q,i}} \right|^2 \quad (14)$$

where Q is query image, Lg is feature vector length, I_1 is image in database; $f_{I,i}$ is i^{th} feature of image I in the database, $f_{Q,i}$ is i^{th} feature of query image Q.

IV. EXPERIMENTAL RESULTS AND DISCUSSIONS

The database DB1 used in our experiment that consists of 116 different textures comprising of 109 textures from Brodatz texture photographic album [28], seven textures from USC database [29]. The size of each texture is 512×512 and is further divided into sixteen 128×128 non-overlapping sub-images, thus creating a database of 1856 (116×16) images.

The performance of the proposed method is measured in terms of average retrieval precision (ARP) and average retrieval rate by following equations.

$$Precision\,(P) = \frac{No.of\ Relevant\ Images\ Retrieved}{Total\ No.of\ Images\ Retrieved} \times 100 \quad (15)$$

$$Group\ Precision\,(GP) = \frac{1}{N_1} \sum_{i=1}^{N_1} P \quad (16)$$

$$Average\ Retrieval\ Precision\,(ARP) = \frac{1}{\Gamma_1} \sum_{j=1}^{\Gamma_1} GP \quad (17)$$

$$Recall\,(R) = \frac{Number\ of\ relevant\ images\ retrieved}{Total\ Number\ of\ relevant\ images} \quad (18)$$

$$Group\ Recall\,(GR) = \frac{1}{N_1} \sum_{i=1}^{N_1} R \quad (19)$$

$$Average\ Retrieval\ Rate\,(ARR) = \frac{1}{\Gamma_1} \sum_{j=1}^{\Gamma_1} GR \quad (20)$$

where N_1 is number of relevant images and Γ_1 is number of groups.

Table II summarizes the retrieval results of the proposed method (M_band_DT_CWT) and other previously available methods in terms of average recall and Table III and Fig. 7 illustrate the performance of proposed method and other available methods in terms of ARR. Table IV summarize the performance of proposed method with energy, standard deviation and combination of them in terms of ARP. Table V and Fig. 7 illustrate the performance of proposed method with different distance measures in terms of average retrieval rate.

From the Tables II to V and Fig. 7 to 8 the following points can be observed:

1. The average retrieval rate (ARR) of the proposed method (75.54%) is more as compared to M_band_DWT (73.81%) and M_band_RWT (74.52%), DT_CWT (74.73%), DT_RCWT (71.17%), GT (74.32%) and (DWT (69.61%).
2. The performance of the proposed method with d_1 distance (75.54%) is more as compared to Canberra (75.36%), Euclidean (62.26%), and Manhattan distance (72.94%).

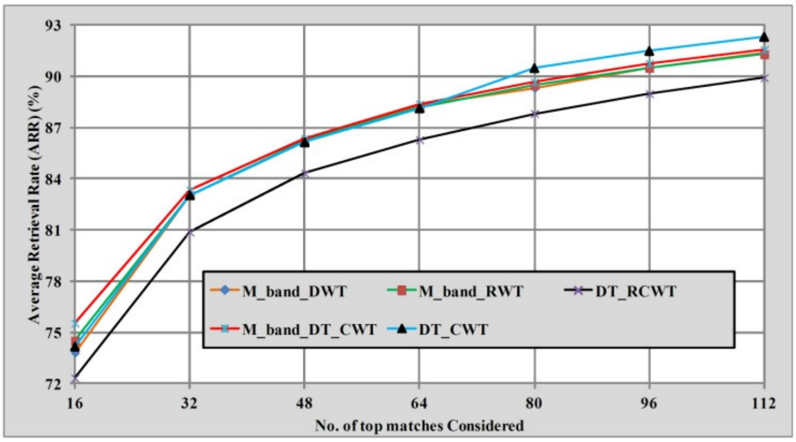

Fig. 7: Comparison of proposed method with other existing methods in terms average retrieval rate.

From Tables II to V, Fig. 7 to 8, and above observations, it is clear that the proposed method is outperforming the M_band_DWT, M_band_RWT, GT, DT-CWT, DT-RCWT and DWT techniques in terms of ARR and ARP. Fig. 9 illustrates the retrieval results of query image based on the proposed method.

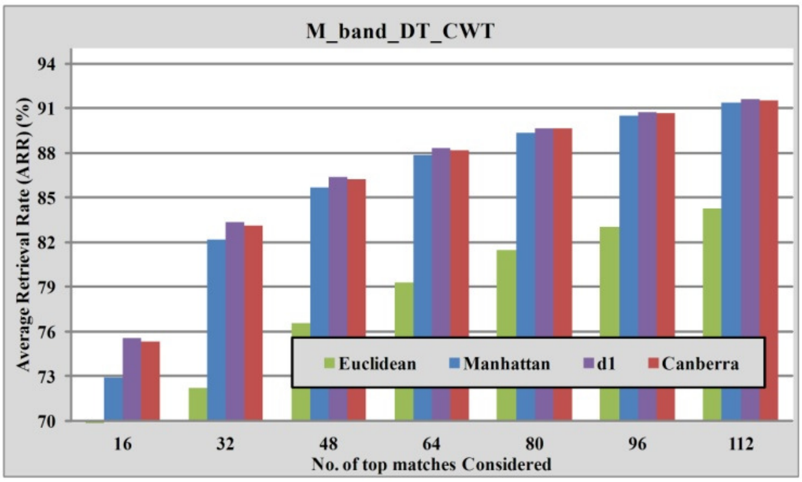

Fig. 8: Performance of proposed method with different distance measures in terms average retrieval rate.

V. M- CHANNEL FILTER BANK

TABLE II Retrieval results of all techniques in terms of average retrieval rate

T1: DT_CWT; T2: DT_RCWT; T3: M_band_DWT; T4: M_band_RWT; PM: M_band_DT_CWT

	GT	DWT	T1	T2	T3	T4	PM
Energy (E)	69.83	67.67	69.01	68.37	71.21	69.10	75.11
Standard Deviation (STD)	59.64	66.70	69.12	64.52	69.74	73.48	73.37
E+STD	74.32	69.61	74.73	71.17	73.81	74.52	75.54

TABLE III Retrieval results of all techniques in terms of average retrieval rate

Method	Number of top matches considered						
	16	32	48	64	80	96	112
M_band_DWT	73.81	83.05	86.14	88.28	89.31	90.47	91.39
M_band_RWT	74.52	83.03	86.21	88.15	89.47	90.49	91.29
DT_CWT	74.16	83.03	86.13	88.11	90.48	91.48	92.3
DT_RCWT	72.33	80.88	84.32	86.28	87.82	88.98	89.92
M_band_DT_CWT	75.54	83.33	86.36	88.36	89.66	90.76	91.56

TABLE IV Retrieval results of Proposed Method in terms of average retrieval Precision

	Number of top matches considered								
	1	3	5	7	9	11	13	15	16
Energy (E)	100	94.61	91.27	88.26	85.67	82.92	80.10	76.84	75.11
Standard Deviation (STD)	100	92.72	89.52	86.75	84.00	81.36	78.32	75.17	73.37
E+STD	100	94.71	91.54	88.85	86.17	83.51	80.66	77.45	75.54

TABLE V Performance of Proposed Method with Different Distance Measures

Method	Distance Measure	Number of top matches considered						
		16	32	48	64	80	96	112
M_band_DT_CWT	Manhattan	72.94	82.20	85.65	87.87	89.36	90.50	91.37
	Canberra	75.36	83.12	86.19	88.20	89.62	90.67	91.51
	Euclidean	62.26	72.19	76.57	79.32	81.46	83.03	84.29
	d1	75.54	83.33	86.36	88.36	89.66	90.76	91.56

VI. CONCLUSIONS

A new image indexing and retrieval algorithm using M_band_DT_CWT is proposed in this paper. The performance of the proposed method is tested by conducting experimentation on Brodatz database. The results after being investigated show a significant improvement in terms of average retrieval rate and average retrieval precision as compared to other existing transform domain techniques.

Further, the performance of the proposed method can be improved by combining the M-band dula tree rotated complex wavelet transform (M_band_DT_RCWT) with the M_band_DT_CWT.

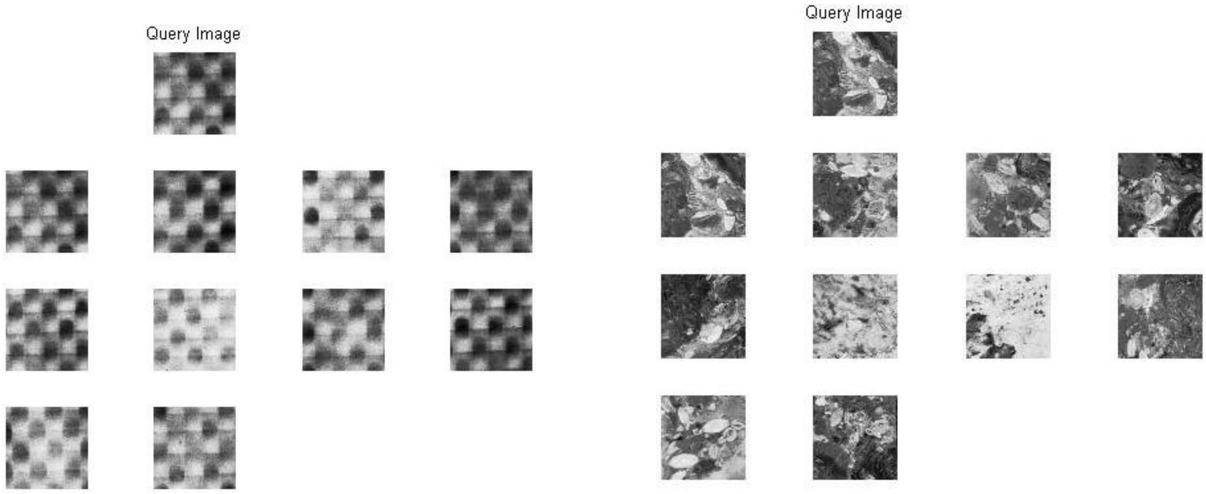

(a) (b)

Fig. 9: Retrieval results of proposed method of query image: (a) 123 and (b) 956

REFERENCE

[1] Y. Rui and T. S. Huang, Image retrieval: Current techniques, promising directions and open issues, J.. Vis. Commun. Image Represent., 10 (1999) 39–62.

[2] A. W.M. Smeulders, M. Worring, S. Santini, A. Gupta, and R. Jain, Content-based image retrieval at the end of the early years, IEEE Trans. Pattern Anal. Mach. Intell., 22 (12) 1349–1380, 2000.

[3] M. Kokare, B. N. Chatterji, P. K. Biswas, A survey on current content based image retrieval methods, IETE J. Res., 48 (3&4) 261–271, 2002.

[4] Ying Liu, Dengsheng Zhang, Guojun Lu, Wei-Ying Ma, Asurvey of content-based image retrieval with high-level semantics, Elsevier J. Pattern Recognition, 40, 262-282, 2007.

[5] Liu, F., Picard, R.W., 1996. Periodicity, directionality, and randomness: Wold features for image modeling and retrieval. IEEE Trans. Pattern Anal. Machine Intell. 18, 722–733.

[6] J. R. Smith and S. F. Chang, Automated binary texture feature sets for image retrieval, Proc. IEEE Int. Conf. Acoustics, Speech and Signal Processing, Columbia Univ., New York, (1996) 2239–2242.

[7] A. Ahmadian, A. Mostafa, An Efficient Texture Classification Algorithm using Gabor wavelet, 25th Annual international conf. of the IEEE EMBS, Cancun, Mexico, (2003) 930-933.M.

[8] M. N. Do and M. Vetterli, "The contourlet transform: An efficient directional multi-resolution image representation," IEEE Trans. Image Process., vol. 14, no. 12, pp. 2091–2106, 2005.

[9] M. Unser, Texture classification by wavelet packet signatures, IEEE Trans. Pattern Anal. Mach. Intell., 15 (11): 1186-1191, 1993.

[10] B. S. Manjunath and W. Y. Ma, Texture Features for Browsing and Retrieval of Image Data, IEEE Trans. Pattern Anal. Mach. Intell., 18 (8): 837-842, 1996.

[11] M. Kokare, P. K. Biswas, B. N. Chatterji, Texture image retrieval using rotated Wavelet Filters, Elsevier J. Pattern recognition letters, 28:. 1240-1249, 2007.

[12] M. Kokare, P. K. Biswas, B. N. Chatterji, Texture Image Retrieval Using New Rotated Complex Wavelet Filters, IEEE Trans. Systems, Man, and Cybernetics, 33 (6): 1168-1178, 2005.

[13] M. Kokare, P. K. Biswas, B. N. Chatterji, Rotation-Invariant Texture Image Retrieval Using Rotated Complex Wavelet Filters, IEEE Trans. Systems, Man, and Cybernetics, 36 (6): 1273-1282, 2006.

[14] L. Birgale, M. Kokare, D. Doye, Color and Texture Features for Content Based Image Retrieval, International Conf. Computer Grafics, Image and Visualisation, Washington, DC, USA, (2006) 146 – 149.

[15] Subrahmanyam, A. B. Gonde and R. P. Maheshwari, Color and Texture Features for Image Indexing and Retrieval, IEEE Int. Advance Computing Conf., Patial, India, (2009) 1411-1416.

[16] Manesh Kokare, P.K. Biswas, B.N. Chatterji, Cosine-modulated wavelet based texture features for content-based image retrieval, Pattern Recognition Letters 25 (2004) 391–398.

[17] R.A. Gopinath, and C.S. Burrus, Wavelets and filter banks, in: C.K. Chui (Ed.), wavelets: A tutorial in theory and applications, Academic Press, San Diego, CA., (1992) 603-654.

[18] Hsin, H.C., 2000. Texture segmentation using modulated wavelet transform. IEEE Trans. Image Process. 9 (7), 1299–1302.

[19] Guillemot, C., Onno, P., 1994. Cosine-modulated wavelets: New results on design of arbitrary length filters and optimization for image compression. In: Proc. Internat. Conf. on Image Processing 1, Austin, TX, USA, pp. 820–824.
[20] S. Mallat, "A Theory for multiresolution signal decomposition: the wavelet representation," IEEE Trans. on Pattern Analysis and Machine Intelligence, 11(7) 674-693, 1989.
[21] O. Rioul and M. Veterli, "Wavelets and signal processing," IEEE Signal Processing Magazine, Vol.8 pp. 14-38, 1991.
[22] I. Daubechies, "Orthonormal bases of compactly supported wavelets", Communications on Pure and Applied Mathematics, Vol. 41, pp 909-996, 1988.
[23] H. Zou, and A.H. Tewfik, "Discrete orthogonal M-band wavelet decompositions," in Proceedings of Int. Conf. on Acoustic Speech and Signal Processing, Vol.4, pp. IV-605-IV-608, 1992.
[24] C. Chaux, L. Duval and J. C. Pesquet. Hilbert pairs of M-band orthonotmal wavelet bases. In Proc. Eur. Sig. and Image Proc. Conf., 2004.
[25] C. Chaux, L. Duval and J. C. Pesquet, "Image analysis using a dual-tree M-band wavelet transform. IEEE Trans. Image Processing, 15 (8): 2397-2412, August 2006.
[26] Hubel, D.H., Wiesel, T.N., 1962. Receptive fields, binocular interaction and functional architecture in the cat's visual cortex. J. Physiol. 160, 106–154.
[27] Daugman, J., 1980. Two-dimensional spectral analysis of cortical receptive field profile. Vision Res. 20, 847–856.
[28] P. Brodatz, "Textures: A Photographic Album for Artists and Designers," New York: Dover, 1996.
[29] University of Suthern California, Signal and Image Processing Institute, Rotated Textures. [Online]. Available: http://sipi.usc.edu/database/.

Authors

K. N. PRAKASH received his Bachelor degree in Electronics and Communication Engineering from Acharya Nagarjuna University, Guntur, India in 1997 and Master of technology in computer Applications from Malnad College of Engineering, Hassan, India in 2001.He is currently pursuing the Ph.D degree in the Department of Electronics and Communication Engineering from Jawaharlal Nehru Technological University Kakinada, India. He has more than 12 years experience of Teaching under graduate and post graduate level. He has published Ten Technical papers in International Journals. He is interested in the areas of signal and Image processing, Microprocessors.

K. Satya Prasad received his Ph.D degree from IIT Madras, India. He is presently working as professor in the Department of Electronics and Communication Engineering, JNTU college of Engineering Kakinada and Rector of Jawaharlal Nehru Technological University, Kakinada, India. He has more than 31 years of teaching and 20 years of research experience. He published 30 research papers in international and 20 research papers in National journals. He guided 8 Ph.D theses and 20 Ph.D theses are under his guidance. He authored Electronic Devices and Circuits text book. He held different positions in his carrer like Head of the Department, Vice Principal, Principal for JNTU Engg College. His area of interests includes Digital Signal and Image Processing, Communications, Ad-hoc networks etc.